Journal of Nano- and Electronic Physics
Vol. **12** No 4, 04007(4pp) (2020)

Журнал нано- та електронної фізики
Том **12** № 4, 04007(4cc) (2020)

Characterization of Crystal Structure and Magnetic Properties of $Zn_{(1-x)}Mn_xO$ (x = 0.086 and 0.090) Nanoparticles Synthesis Results Using Coprecipitation Method

Heru Harsono*

Department of Physics, Faculty of Mathematics and Natural Sciences, Brawijaya University, 65145 Malang, Indonesia

(Received 15 April 2020; revised manuscript received 15 August 2020; published online 25 August 2020)

$Zn_{(1-x)}Mn_xO$ (x = 0.086 and 0.090) nanoparticles have been successfully synthesized. This research aims to make $Zn_{(1-x)}Mn_xO$ nanoparticles and observe the effect of Mn^{2+} doping ion concentration in ZnO material by coprecipitation method, which is then followed by heat treatment at 350 °C for 3 h. $Zn_{(1-x)}Mn_xO$ nanoparticles produced were then characterized using XRD, SEM, VSM and FTIR equipment. XRD data were generated using the Rietveld program. The XRD refinement results show that the substitution of Mn^{2+} ions into ZnO can change the behavior of the lattice parameters and atomic density. The shape and particle size of $Zn_{(1-x)}Mn_xO$ nanoparticle samples change with the addition of Mn^{2+} ion doping. Likewise, there is a change in magnetic properties such as magnetic remanent (M_r) of $Zn_{(1-x)}Mn_xO$ nanoparticles as a result of substitution with the addition of Mn^{2+} ions.

Keywords: $Zn_{(1-x)}Mn_xO$ nanoparticles, Coprecipitation, Structure parameters, Magnetic properties.

DOI: 10.21272/jnep.12(4).04007 PACS numbers: 61.46.Df, 75.75.Fk

1. INTRODUCTION

Zinc oxide nanoparticles are one of the semiconductor nanoparticle materials that have been widely developed in nanotechnology because they have mechanical, electrical and optical properties that can be applied for many uses including solar cells, catalysts, ultraviolet protective thin films, gas sensors, and others.

There are many ways to synthesize zinc oxide nanoparticles which include coprecipitation methods [1, 2], solid-state reaction [3, 4], ion implantation [5], solvo-thermal process [6, 7], and diluted magnetic semiconductors (DMS) which attracted many researchers because of their potential applications in spintronic devices. They can be utilized as spin-valve transistors, spin light-emitting diodes, non-volatile memory, optical isolators and so on. Inside doped DMS there are the transition metals of groups II-VI and III-V [8]. Wurtzite zinc oxide with wide gap energy (3.4-3.7 eV) is a material that attracts attention [9, 10]. Some zinc (Zn) can be substituted with manganese (Mn) ions which can give ferromagnetic properties [11]. The solubility of Mn ions to the ZnO lattice causes the availability of carrier atoms which increases the ferromagnetic properties of ZnO at room temperature [12]. Of all transition metals, Mn doping in ZnO gives the best results because Mn has a low Curie temperature (Tc) and the radius of Mn atom approaches the radius of Zn atom so that it is easily fabricated when compared to other transition materials [13]. Zinc oxide hexagonal wurtzite crystal is a promising material for photodetectors, blue laser diodes and ultraviolet. Many studies have been carried out to produce the ferromagnetic properties of zinc oxide including powder and thin films.

The synthesis of manganese doped ZnO nanoparticles by the coprecipitation method without the presence of a secondary phase produces good ferromagnetic properties in the sample [14]. In this research, Mn atom doping (0.086 and 0.090) was carried out to further reveal the behavior of magnetic properties that have potential applications for spintronic devices.

2. EXPERIMENTAL

2.1 Materials

Materials with a high level of purity such as $Zn(CH_3COO)_2.2H_2O$, $Mn(CH_3COO)_2.4H_2O$, HCl 37 %, NH_4OH 25 % from the catalog of Merck Germany are used in this research.

$Zn_{(1-x)}Mn_xO$ (x = 0.086 and 0.090) sample is created using chemical coprecipitation method. The basic materials are $Zn(CH_3COO)_2.2H_2O$ and $Mn(CH_3COO)_2.4H_2O$. They are mixed and dissolved together with a predetermined stoichiometry into HCl 0.5 M, then NH_4OH 3 M is slowly added into the solution mixture until the pH of the solution reaches 9, and it is stirred using a magnetic stirrer while heating it to a temperature of 85 °C for 6 h. After that, the solution is washed with distilled water until the pH lowers to 7. The precursors are dried in an oven at 100 °C for 3 h and then calcined in a furnace at 350 °C for 3 h.

2.2 Characterization

The samples of $Zn_{(1-x)}Mn_xO$ (x = 0.086 and 0.090) nanoparticles produced are characterized by X-ray diffraction (XRD) using Phillips X-pert Powder Diffractometer with a CuKα radiation source (λ = 1.54056 Å). The analysis of the diffraction patterns by the Rietveld refinement method using the Rietica program is carried out to extract crystal structure information from $Zn_{(1-x)}Mn_xO$ (x = 0.086 and 0.090) synthesized samples. Scanning Electron Microscopy (SEM, FEI Inspect S50) photos are completed with Energy Dispersive Spectrophotometer (EDS), and $Zn_{(1-x)}Mn_xO$ (x = 0.086 and 0.090) samples are used to study morphological characteristics and element mapping. Meanwhile, FTIR analysis using the Shimadzu FTIR-8400 S spectrophotometer is carried

* heru_har@ub.ac.id

out to measure the absorption peaks associated with the vibrational frequencies of the bonds of the atoms making up $Zn_{(1-x)}Mn_xO$ ($x = 0.086$ and 0.090) nanoparticles. Magnetic properties analysis is performed using Vibrating Sample Magnetometer (VSM).

3. RESULTS AND DISCUSSION

3.1 Analysis of the Crystal Structure

The XRD data of the sample are shown in Fig. 1. All samples show a hexagonal structure with a P63/mc space group. The parameters of R_p, R_{wp}, and χ^2 obtained after refinement for all samples are listed in Table 1.

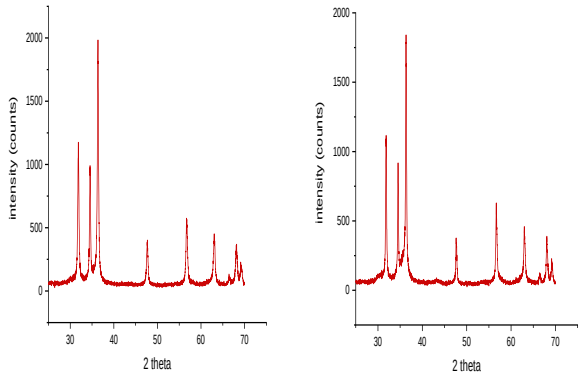

Fig. 1 – The profile of XRD patterns of $Zn_{(1-x)}Mn_xO$ nanoparticles: (a) $x = 0.086$ and (b) $x = 0.090$

Table 1 – Parameters of $Zn_{(1-x)}Mn_xO$ ($x = 0.086$ and $x = 0.090$) nanoparticle structure

No.	Parameters	$x = 0.086$	$x = 0.090$
1	Lattice parameter $a = b$ (Å)	3.2533	3.2489
2	Lattice parameter c (Å)	5.2073	5.1988
3	ρ (g/cm^3)	5.663	5.620
4	ZnO phase (%)	100	100

From Table 1 it can be seen that the lattice parameters a and c are reduced after Mn^{2+} ion substitution. This shows that the hexagonal structure has contracted along the a-axis and the c-axis. The decrease in the lattice parameters ($a = b$ and c) is closely related to the covalent radius of the Mn^{2+} ion. A small shift in the value of the lattice parameter and the volume of the crystal indicates the successful incorporation of Mn^{2+} ions into ZnO nanoparticles.

3.2 FTIR Analysis

Fig. 2 shows the observation result of samples with FTIR using spectroscopy FTIR-8400S Shimadzu with the range of wavenumber between 400-4000 cm^{-1}.

Table 2 represents the quantity of absorption peak values and the functional groups for all variations of manganese doping concentrations. There are two main absorption peaks with a wide band in the wavenumber region of around 1600 cm^{-1} and 1400 cm^{-1} which are absorption bands from stretching vibrations of the carboxyl group (C=O) [15] and Zn–C–O vibrations [16].

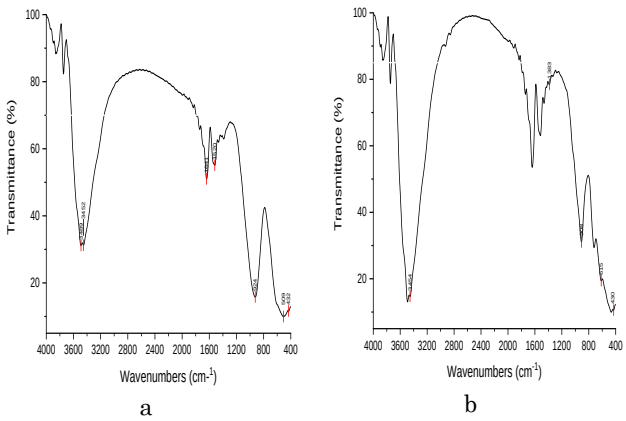

Fig. 2 – FTIR spectrum of $Zn_{(1-x)}Mn_xO$ nanoparticles: (a) $x = 0.086$ and (b) $x = 0.090$

The authors of [17] obtained two main wide absorption bands in the wavenumber region of 1650 cm^{-1} and 1400 cm^{-1} which are related to asymmetric and symmetric stretching vibrations of the carboxyl groups (C=O) located on the surface of nanoparticles originating from atmospheric CO_2. The absorption peak at the wavenumber region of around 3500 cm^{-1} represents stretching vibration of O–H [18], and [19] stated that absorption in the wavenumber region of around 3428 cm^{-1} is the O–H vibrational mode of Cu-doped ZnO nanoparticles. The O–H vibrational mode is also obtained at a wavenumber of around 3390 cm^{-1} [20] and 900 cm^{-1} according to the deformation C=O [21]. Absorption peak in the wavenumber region of around 2300 cm^{-1} is owned by CO_2 vibrations due to their presence in the air [15]. Another peak is observed in the wavenumber region of around 650 cm^{-1} which is owned by symmetric bending vibrations from O–H [18]. Most importantly, a very strong band is detected in the wavenumber region at 487.96 cm^{-1} in the FTIR spectrum for ZnO without doping which is claimed to be in accordance with the vibrational strain of Zn–O [18]. Other peaks in the wavenumber region of around 500 cm^{-1} and 400 cm^{-1} in the FTIR spectrum for Mn-doped ZnO clearly reveal the existence of strain vibrations between transition metals (Zn, Mn) and O [18, 22]. Some researchers claim that absorption around the wavenumber is the stretching vibrations of Zn–O, such as around 420 cm^{-1} [19], around 460 cm^{-1} [20], around 410-438 cm^{-1}, Ghotbi, et al. (2011). The absorption peaks (Zn, Mn)–O decrease along with increasing manganese doping. Ultimately, these absorption peaks indicate the presence of resonant interactions among the vibrational modes of oxide ions in $Zn_{(1-x)}Mn_xO$ nanoparticles.

3.3 SEM-EDS Analysis

As can be seen in Fig. 3a, SEM characterization results show that the particle size for all samples is in the order of nanometers. Morphology and particle size are found to be porous and non-uniform and agglomeration occurs. After substitution of Mn by 0.086, the majority of particles are rod, while the majority of particles are hexagonal rod for Mn substitution by 0.090. The growth of wurtzite grain is inhibited by the incorporation of Mn^{2+} ions. However, the grain size of $Zn_{(1-x)}Mn_xO$ ($x = 0.086$ and $x = 0.090$) nanoparticles is relatively stable.

Table 2 – Functional groups of $Zn_{(1-x)}Mn_xO$ ($x = 0.086$ and $x = 0.090$) nanoparticles

Wave absorption (cm^{-1})	Functional group						
The concentration of Mn doping	O–H stretching	CO_2 vibration	C=O stretching	Zn–C–O vibration	C=O deformation	O–H sym. bending	Zn–O stretching
0.086	3.489	absent	1.641	1.389	924	509	432
0.090	3.454	absent	1.641	1.383	908	615	430

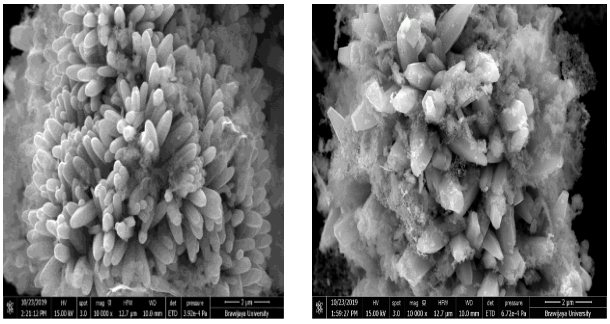

a b

Fig. 3 – SEM micrographs of $Zn_{(1-x)}Mn_xO$ nanoparticle samples: (a) $x = 0.086$ and (b) $x = 0.090$

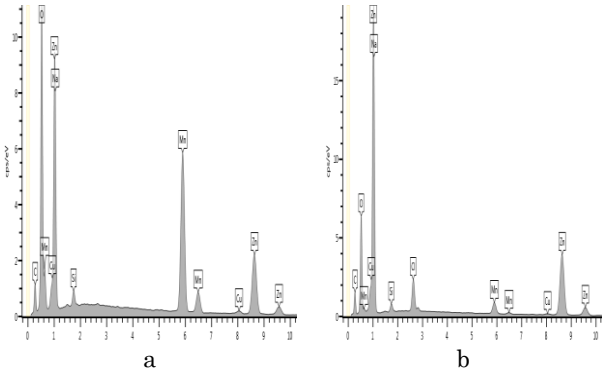

a b

Fig. 4 – EDS spectrum of $Zn_{(1-x)}Mn_xO$ nanoparticle samples: (a) $x = 0.086$ and (b) $x = 0.090$

Table 3 – Distribution of elements in $Zn_{(1-x)}Mn_xO$ ($x = 0.086$ and $x = 0.090$) nanoparticles

No	Element	$x = 0.086$	$x = 0.090$
1	O	50.3	37.1
2	Zn	11.0	17.4
3	Mn	11.9	1.3

The SEM photo clearly illustrates that the morphology of the sample is not homogeneous with the non-uniform distribution. Different particles cannot be distinguished very clearly due to the growth of grains. Based on Fig. 3 it is also clear that the particles are clustered together. This is due to the low calcination temperature so that the liquid bridge, which is caused by atomic diffusion, has not been formed.

The elements contained in $Zn_{(1-x)}Mn_xO$ nanoparticles are identified using Energy Dispersive Spectrophotometer (EDS) equipment incorporated into SEM. The spectrum of EDS observations is shown in Fig. 4. Meanwhile, the elements contained in $Zn_{(1-x)}Mn_xO$ are listed in Table 3.

In Fig. 4, the peaks of zinc (Zn) element, oxygen (O) element, and manganese (Mn) element are observed. Observation of these peaks confirms the presence of the manganese element in ZnO nanoparticle samples with various doping concentrations.

Based on Table 3, it appears that the comparison between Zn and Mn elements (in % of atoms) for each sample has a different content, but the difference is not too significant.

3.4 Analysis of Magnetic Properties

The magnetic behavior of $Zn_{(1-x)}Mn_xO$ ($x = 0.086$ and $x = 0.090$) nanoparticles was measured at room temperature using VSM. From the results of magnetization measurements of $Zn_{(1-x)}Mn_xO$ ($x = 0.086$ and $x = 0.090$) nanoparticles using VSM, a hysteresis curve slowing the characteristics of the ferromagnetic sample is obtained, as shown in Fig. 5. Ferromagnetic materials have a resultant large atomic magnetic field. This is caused by the magnetic moment of the electron spin.

In this material, there are many unpaired electron spins. Each unpaired electron spin will create a magnetic field so that the total magnetic field generated by one atom becomes larger. The magnetic field of each ferromagnetic material atom is very strong, and therefore the interaction between neighboring atoms causes most atoms to align themselves to form groups known as domains. Before being given an external magnetic field, ferromagnetic material has a domain with a strong magnetic moment, but this magnetic moment has a different direction from one domain to another. Therefore, the magnetic fields produced by each domain cancel each other out. If this material is given an external magnetic field, these domains will align themselves in the direction of the external magnetic field. The stronger the magnetic field, the more domains that align themselves. As a result, the magnetic field in the ferromagnetic material is getting stronger. After all, domains have been directed, the addition of an external magnetic field does not effect because there are no more domains to be rectified. This situation is called saturation. A high remanent magnetization value is obtained by $Zn_{(1-x)}Mn_xO$ ($x = 0.090$) nanoparticles in Fig. 5. The remanent magnetization value is proportional to the coercivity field which tends to rise.

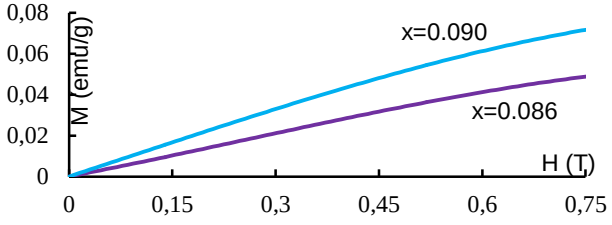

Fig. 5 – Test results of vibrating sample magnetometer of $Zn_{(1-x)}Mn_xO$ ($x = 0.086$ and $x = 0.090$) nanoparticles

4. CONCLUSIONS

$Zn_{(1-x)}Mn_xO$ ($x = 0.086$ and 0.090) nanoparticles have been successfully synthesized by the coprecipitation method. The observation results of samples using FTIR showed the presence of Zn–O stretching modes in the hexagonal lattice observed in the spectrum at 430 cm^{-1} and 432 cm^{-1}. This confirms the formation of hexagonal structures. Changes in the structural parameters, morphology and magnetic properties of $Zn_{(1-x)}Mn_xO$ ($x = 0.086$ and 0.090) nanoparticle samples are characterized using XRD, SEM-EDS, and VSM equipment.

The XRD refinement results show that the influence of Mn^{2+} ion doping causes the shrinkage of the lattice parameter on the behavior of crystal structures. The morphology of $Zn_{(1-x)}Mn_xO$ ($x = 0.086$ and 0.090) nanoparticle samples is changing in size and shape. In addition, magnetic behavior such as remanent magnetization (M_r) decreases due to increasing Mn^{2+} ion doping. From the results of a series of tests, it can be stated that $Zn_{(1-x)}Mn_xO$ ($x = 0.086$ and 0.090) nanoparticle samples can be applied as the basis of spintronic equipment.

ACKNOWLEDGEMENTS

Acknowledgement is given to the Rector of Brawijaya University who has funded this research for the Grand for Doctoral Program.

REFERENCES

1. M. Bououdina, K. Omri, A. El Amiri, O.M. Lemine, A. Alyamani, E.K. Hill, H. Lassri, L. Elk Mir, *Physica E* **56**, 107 (2014).
2. S. Fabbiyola, L.J. Kennedy, A.A. Dakhel, M. Bououdina, J.J. Vijaya, T. Ratnaji, *J. Molec. Struct.* **1109**, 89 (2016).
3. O.D. Jayakumar, I.K. Gopalakrishnan, R.M. Kadam, A. Vinu, A. Asthana, A.K. Tyagi, *J. Crystal Growth* **300**, 358 (2007).
4. D. Milivojevic, J. Blanusa, V. Spasojevic, V. Kusigerki, B. Babic-Stojic, *Solid State Commun.* **141**, 641 (2007).
5. R. Sanz, J. Jensen, G. Gonsalez-Diaz, O. Martinez, M. Vasquez, M. Hernadez-Velez, *Res. Lett.* **4**, 878 (2009).
6. S. Banerjee, K. Rajendran, N. Gayathri, M. Sardar, S. Senthilkumar, V. Sengodan, *J. Appl. Phys.* **104**, 043913 (2008).
7. T. Ghosal, S. Kar, S. Biswas, S.K. De, P.M.G. Nambissan, *J. Phys. Chem. C* **113**, 3419 (2009).
8. S.W. Jung, S.J. An, Y. Gyu-Chul, *Appl. Phys. Lett.* **80**, 4561 (2002).
9. S. Chattopadhyay, S. Dutta, A. Banerjee, D. Jana, S. Bandyopadhyay, A. Sarkar, *Physica B* **404**, 1509 (2009).
10. M. Chaari, A. Matoussi, Z. Fakhfakh, *Mater. Sci. Appl.* **2**, 765 (2011).
11. K.J. Kim, Y.R. Park, *Appl. Phys. Lett.* **81**, 1420 (2002).
12. J.H. Yang, L.Y. Zhao, Y.J. Zhang, Y.X. Wang, H.L. Liu, M.B. Wei, *Solid State Commun.* **143**, 566 (2007).
13. P. Moontragoon, S. Pinitsoontorn, P. Thongbai, *Microelectron. Eng.* **108**, 158 (2013).
14. H. Harsono, I.N.G. Wardana, A.A. Sonief, Darminto, *J. Nano Res.* **35**, 67 (2016).
15. M.E. Abrishami, S.M. Hosseini, AE.A. Kakhki, A. Kompany, M. Ghasemifard, *Int. J. Nanosci.* **9**, 19 (2010).
16. S. Bagheri, K.G. Chandrappa, S.B.A. Hamid, *De Pharma Chemica* **5** No 3, 265 (2013).
17. S. Senthilkumar, K. Rajendran, S. Banerjee, T.K. Chin, V. Sengoda, *Mater. Sci. Semicond. Proc.* **11** No 1, 265 (2008).
18. B.N. Dole, V.D. Mote, V.R. Huse, Y. Purushotham, M.K. Lande, K.M. Jadhav, S.S. Shah, *Curr. Appl. Phys.* **11**, 762 (2011).
19. A.J. Reddy, M.K. Kokila, H. Nagabhushana, R.P.S. Chakradhar, C. Shivakumara, J.L. Rao, B.M. Naghabushana, *J. Alloy. Compd.* **509**, 5349 (2011).
20. M. Makkar, H.S. Bathti, *Chem. Phys. Lett. B* **507**, 122 (2011).
21. J. Alaria, P. Turek, M. Bernard, M. Bouloudenine, A. Berbadj, N. Brihi, G. Schmerber, S. Colis, A. Dinia, *Chem. Phys. Lett.* **415**, 337 (2005).
22. J.Y. Kwon, K.H. Kim, C.S. Lim, *J. Ceram. Proc. Res.* **3**, 146 (2002).

Характеристика кристалічної структури та магнітних властивостей результатів синтезу наночастинок $Zn_{(1-x)}Mn_xO$ ($x = 0{,}086$ та $0{,}090$), отриманих за допомогою методу співосадження

Heru Harsono

Department of Physics, Faculty of Mathematics and Natural Sciences, Brawijaya University, Malang 65145, Indonesia

Наночастинки $Zn_{(1-x)}Mn_xO$ ($x = 0{,}086$ та $0{,}090$) були успішно синтезовані. Це дослідження має на меті виготовлення наночастинок $Zn_{(1-x)}Mn_xO$ та спостерігання впливу концентрації легуючих іонів Mn^{2+} у матеріалі ZnO методом співосадження, за яким слідує термічна обробка при 350 °C протягом 3 год. Потім отримані наночастинки $Zn_{(1-x)}Mn_xO$ характеризували з використанням технологій XRD, SEM, VSM та FTIR. Дані XRD були отримані за допомогою програми Рітвельда. Результати уточнення XRD показують, що заміщення іонів Mn^{2+} в ZnO може змінити поведінку параметрів решітки та атомну густину. Форма та розмір частинок зразків $Zn_{(1-x)}Mn_xO$ змінюються з додаванням легуючих іонів Mn^{2+}. Так само відбувається зміна магнітних властивостей, таких як магнітний залишок (M_r) наночастинок $Zn_{(1-x)}Mn_xO$, в результаті заміщення з додаванням іонів Mn^{2+}.

Ключові слова: $Zn_{(1-x)}Mn_xO$ наночастинки, Співосадження, Параметри структури, Магнітні властивості.